

Unusual Co-Crystallization of both Monomeric and Dimeric Forms of Cu[PhN(py)quin]Cl₂

John J. Allen · Andrew R. Barron

Received: 10 August 2010 / Accepted: 30 December 2010 / Published online: 14 January 2011
© Springer Science+Business Media, LLC 2011

Abstract The aryl functionalized diquinolyl amine MesN(quin)₂ (**1**) and the pyridyl-quinolyl amine (2,6-iPr₂C₆H₃)N(py)quin (**2**) have been prepared via palladium catalyzed cross-coupling of substituted anilines with 2-chloro-quinoline. The HBF₄ acid salts of (2,6-iPr₂C₆H₃N(quin)₂ (**3**) and MesN(py)quin (**4**), as well as the copper complex [Cu{PhN(py)quin}Cl₂] (**5**) have been prepared in order to probe the effect that ligand coordination has on its geometry. The molecular structures of each have been determined by X-ray crystallography. The free ligands **1** and **2** crystallize in three-bladed propellar conformations, having smaller degrees of “pitch” between the two heterocycles than either has with the aryl “blade”, allowing for greater heterocycle π -system overlap with the amine lone pair. Acid confinement of similar ligands in **3** and **4** results in forced coplanarity of the two heterocycles, which coordinate the HBF₄ proton in an asymmetric fashion. The copper complex **5** crystallizes with both monomeric and dimeric forms present in the asymmetric unit. Crystal data: (**1**) Space group P2₁/c, $a = 14.058(3)$, $b = 12.202(2)$, $c = 12.831(3)$ Å, $\beta = 104.61(3)$ °, $V = 2129.8(8)$ Å³, $Z = 4$, $R = 0.0596$, $wR_2 = 0.1453$. (**2**) Space group P2₁/c, $a = 22.250(4)$, $b = 8.628(2)$,

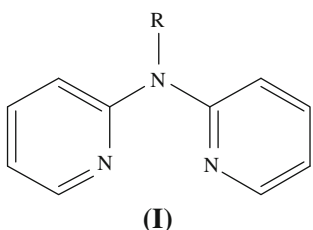
$c = 23.031(5)$ Å, $\beta = 92.88(3)$ °, $V = 4370(2)$ Å³, $Z = 8$, $R = 0.0514$, $wR_2 = 0.1323$. (**3**) Space group Pbca, $a = 13.886(3)$, $b = 18.016(4)$, $c = 21.347(4)$ Å, $V = 5340(2)$ Å³, $Z = 8$, $R = 0.0722$, $wR_2 = 0.1635$. (**4**) Space group P2₁/c, $a = 10.629(2)$, $b = 18.489(4)$, $c = 10.907(2)$ Å, $\beta = 92.88(3)$, $V = 2140.6(7)$ Å³, $Z = 4$, $R = 0.0551$, $wR_2 = 0.1531$. (**5**) Space group P1̄, $a = 9.706(2)$, $b = 11.325(2)$, $c = 17.322(4)$ Å, $\alpha = 98.28(3)$, $\beta = 94.85(3)$, $\gamma = 91.83(3)$ °, $V = 1875.6(7)$ Å³, $Z = 1$, $R = 0.0481$, $wR_2 = 0.0946$.

Keywords Copper · Quinolyl · Amine · Monomer · Dimer · Co-crystallization

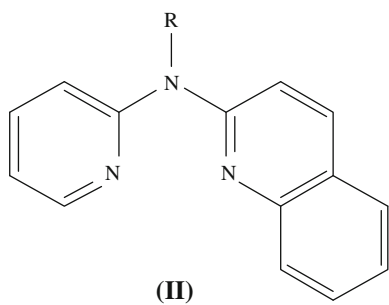
Introduction

We have recently reported a range of aryl substituted *bis*-(2-pyridyl) amine compounds (**1**) and complexes thereof [**1**]. Specifically, HBF₄ acid salts, as well as copper complexes [Cu{RN(py)₂}Cl₂] and [Cu(Ar-dpa)(olefin)]X were prepared in order to examine the effects of coordination on ligand geometry. Through this work, we observed that the reaction of RN(py)₂ (R = Ph, iPrC₆H₄, and 2-naph) with [Cu(MeCN)₄]BF₄, in the presence of HCl, resulted in the formation of the appropriate Cu(II) complex; [Cu{RN(py)₂}Cl₂]. The resulting solid state structures, determined by X-ray crystallography, were found to be dimeric, with a slightly asymmetric Cu(μ -Cl)₂Cu core. This asymmetry is due in part to a trigonal bipyramidal geometry about the copper center, such that one of the bridging chlorides occupies an axial position, while the other takes an equatorial position. The core geometry, however, showed only slight variation between the three dimers, regardless of the identity of the aryl substituent.

J. J. Allen · A. R. Barron (✉)
Department of Chemistry, Rice University,
Houston, TX 77005, USA
e-mail: arb@rice.edu
URL: www.rice.edu/barron



We have also reported the synthesis and molecular structures of both RN(py)quin (**II**) and RN(quin)₂ [2, 3]. In order to understand any change concerning steric interactions with the ancillary ligand in copper(I)-olefin complexes, specifically those brought on by substitution remotely from the metal center, the present study investigates the formation of two new aryl-functionalized di-heterocyclic(amine) ligands, two HBF₄ acid salts of structurally similar ligands, as well as a quinolyl analog, Cu[PhN(py)quin]Cl₂, of the bridged chloro-complexes [1]. Each of which we have synthesized and determined the solid state structures by X-ray crystallography.



Experimental

All reagents in this study were used as received from commercial suppliers and were stored under an argon atmosphere in a drybox. All solvents were distilled and degassed via freeze-pump-thaw immediately prior to use. Glassware was thoroughly cleaned and dried prior to use. With the exceptions of syntheses for **3–5**, all manipulations were performed under an argon atmosphere using standard schlenk line techniques. Free ligands PhN(py)quin, MesN(py)quin (Mes = 2,4,6-Me₃C₆H₂), and (2,6-ⁱPr₂C₆H₃)N(quin)₂ were prepared according to previously established methods [2, 3]. Precursor complex [Cu(MeCN)₄]BF₄ was prepared according to Hathaway et al. [4]. ¹H NMR and ¹³C NMR spectra were obtained at room temperature using Bruker Avance 400 and 500 MHz spectrometers. Chemical shifts are reported relative to internal solvent resonances. IR spectra were obtained using a Nicolet FTIR spectrometer equipped with ATR accessory.

Thermogravimetric analyses were performed on a Seiko I TG/DTA 200 under an argon gas flow of 10–15 mL min⁻¹. GC–MS analyses were performed using Agilent Technologies 5973 network mass selective detector, equipped with 6890 N network GC system.

N-(2,4,6-Trimethyl)phenyl-*N,N*-(2,2'-diquinolyl)amine (**1**)

In a drybox, KO^tBu (785 mg, 7.0 mmol), allyl[1,3-bis(2,6-diisopropylphenyl)-imidazol-2-ylidene]palladium(II)chloride (70 mg, 0.12 mmol), and 2-chloroquinoline (818 mg, 5.0 mmol) were added to a Schlenk flask. To this was added toluene (10 mL) followed by 2,4,6-trimethylaniline (338 mg, 2.5 mmol). The reaction was stirred under nitrogen at 70 °C for 120 h. After cooling, Et₂O (25 mL) was added to the reaction mixture and then washed twice with brine. The organic phase was dried over sodium sulfate before removing solvent in vacuo. The crude product was purified by flash chromatography on silica gel (eluent: 10% ethyl acetate in hexanes). The product was dissolved in hot hexanes and allowed to cool to room temperature. Subsequent cooling to –12 °C over several days resulted in the formation of crystals suitable for diffraction. Yield: 0.191 g (19%), 96% pure by GC–MS. Mp (TGA; sublim.): 254–256 °C. MS (EI,%): *m/z* 389 (M⁺, 46), 374 (M⁺–Me, 100). FTIR (neat, ATR, cm^{−1}): 3133 (w, aromatic ν_{C-H}), 3052 (w, aromatic ν_{C-H}), 3015 (w, aromatic ν_{C-H}), 2988 (w, alkyl ν_{C-H}), 2946 (w, alkyl ν_{C-H}), 2913 (m, alkyl ν_{C-H}), 2853 (w, alkyl ν_{C-H}), 1617 (m), 1595 (s), 1562 (m), 1502 (s, aromatic $\delta_{C=C}$), 1466–1384 (s, aromatic $\delta_{C=C}$), 1344 (m), 1327 (s, 3° aromatic ν_{C-N}), 1293 (s), 1267 (m), 1154 (m), 1118 (m), 1009 (w), 950 (w), 825 (s). ¹H NMR (CD₂Cl₂) 8.00 [2H, d, *J*(H–H) = 8.9 Hz, CH, 4-quin], 7.74 [2H, ddd, *J*(H–H) = 8.1 Hz, *J*(H–H) = 1.5 Hz, *J*(H–H) = 0.7 Hz, CH, 9-quin], 7.69 [2H, ddd, *J*(H–H) = 8.5 Hz, *J*(H–H) = 1.3 Hz, *J*(H–H) = 0.7 Hz, CH, 6-quin], 7.58 [2H, ddd, *J*(H–H) = 8.5 Hz, *J*(H–H) = 6.9 Hz, *J*(H–H) = 1.5 Hz, CH, 7-quin], 7.39 [2H, ddd, *J*(H–H) = 8.1 Hz, *J*(H–H) = 6.9 Hz, *J*(H–H) = 1.3 Hz, CH, 8-quin], 7.30 [2H, d, *J*(H–H) = 8.9 Hz, CH, 3-quin], 7.04 (2H, s, *m*-CH), 2.39 (3H, s, *p*-CH₃), 2.05 (6H, s, *o*-CH₃). ¹³C NMR (CD₂Cl₂): δ 155.91, 147.87, 139.23, 138.23, 138.18, 137.41, 130.13, 129.86, 128.15, 127.79, 125.87, 124.85, 116.68, 21.43, 18.75.

N-(2,6-Diisopropyl)phenyl-*N*-(2-pyridyl)-*N*-(2-quinolyl)amine (**2**)

2-chloroquinoline (1.00 g, 6.0 mmol), *N*-(2,6-diisopropyl)phenyl-*N*-(2-pyridyl)amine (1.27 g, 5.0 mmol), sodium

tert-butoxide (0.75 g, 7.8 mmol), and allyl[1,3-bis(2,6-diisopropylphenyl)-imidazol-2-ylidene]palladium(II)chloride (91 mg, 0.16 mmol) were placed in a Schlenk flask in a drybox. The flask was removed, and toluene (100 mL) was added via cannula. The reaction was stirred under an argon atmosphere at 80 °C for 5 days. After cooling to room temperature, CH₂Cl₂ (100 mL) was added, and the mixture was extracted twice with brine solution. The solvent was removed from the organic phase under reduced pressure, and the resulting residue was purified by column chromatography on silica gel (eluent: 2.5% ethyl acetate in hexanes). Recrystallization from a very slow (ca. 8 months) evaporation of a 1:1 mixture of Et₂O and EtOH gave translucent yellow plates suitable for diffraction. Yield: 0.75 g (39%), 97% pure by GC–MS. Mp (TGA; sublim.): 210–212 °C. MS (EI, %): *m/z* 381.2 (M⁺, 1.0), 338.2 (M⁺–ⁱPr, 100). FTIR (neat, ATR, cm^{−1}): 3058 (w, aromatic ν_{C–H}), 2969 (s, alkyl ν_{C–H}), 2931 (w, alkyl ν_{C–H}), 2912 (w, alkyl ν_{C–H}), 2877 (m, alkyl ν_{C–H}), 2649 (w, vbr), 1637 (w), 1598–1433 (s, aromatic δ_{C=C}), 1366 (m), 1331 (s, 3° aromatic ν_{C–N}), 1299 (w), 1229 (m), 1157 (m), 1045 (s, ν_{B–F}), 823 (s), 759 (s). ¹H NMR (CD₃OD): δ 8.58 [2H, d, *J*(H–H) = 9.3 Hz, CH, 4-quin], 8.39 [2H, dd, *J*(H–H) = 8.3 Hz, *J*(H–H) = 0.8 Hz, CH, 6-quin], 8.08 [2H, dd, *J*(H–H) = 8.0 Hz, *J*(H–H) = 1.3 Hz, CH, 9-quin], 8.08 [2H, ddd, *J*(H–H) = 8.3 Hz, *J*(H–H) = 7.1 Hz, *J*(H–H) = 1.3 Hz, CH, 7-quin], 7.80 [1H, t, *J*(H–H) = 8.2 Hz, *p*–CH, Ph], 7.78 [2H, ddd, *J*(H–H) = 8.0 Hz, *J*(H–H) = 7.1 Hz, *J*(H–H) = 0.8 Hz, CH, 8-quin], 7.66 [2H, d, *J*(H–H) = 8.2 Hz, *m*–CH, Ph], 6.87 [2H, d, *J*(H–H) = 9.3 Hz, CH, 3-quin], 2.90 [2H, sept, *J*(H–H) = 6.8 Hz, CH(CH₃)₂], 1.09 [12 H, d, *J*(H–H) = 6.8 Hz, CH(CH₃)₂]. ¹³C NMR (CD₃OD): δ 155.23, 148.72, 144.45, 141.43, 134.57, 133.55, 133.42, 129.78, 128.99, 128.12, 126.35, 125.03, 115.06, 29.85, 24.41.

(*N*-Mesityl-*N*-(2-pyridyl)-*N*-(2-quinolyl)amine)hydrogen Tetrafluoroborate (**4**)

This compound was prepared in an analogous manner to that of **3**, using MesN(py)quin (0.339 g, 1.0 mmol) as ligand. Yield: 0.191 g (45%) colorless crystals. Mp (TGA; decomp.): 197–199 °C. FTIR (neat, ATR, cm^{−1}): 3120 (m, aromatic ν_{C–H}), 3061 (w, aromatic ν_{C–H}), 2983 (w, alkyl ν_{C–H}), 2926 (m, alkyl ν_{C–H}), 2858 (w, alkyl ν_{C–H}), 2736 (w), 2645 (w, vbr), 1624 (s), 1597 (s), 1506–1437 (s, aromatic δ_{C=C}), 1364 (3° aromatic ν_{C–N}), 1321 (m), 1267 (m), 1149 (m), 1031 (s, ν_{B–F}), 831 (s), 762 (s). ¹H NMR (CD₃OD): δ 8.81 [1H, ddd, *J*(H–H) = 5.4 Hz, *J*(H–H) = 1.9 Hz, *J*(H–H) = 0.9 Hz, CH, 6-py], 8.57 [1H, dd, *J*(H–H) = 9.4 Hz, *J*(H–H) = 0.7 Hz, CH, 4-quin], 8.32 [1H, ddd, *J*(H–H) = 8.5 Hz, *J*(H–H) = 1.5 Hz, *J*(H–H) = 0.8 Hz, CH, 9-quin], 8.07 [1H, ddd, *J*(H–H) = 8.4 Hz, *J*(H–H) = 7.3 Hz, *J*(H–H) = 1.9 Hz, CH, 4-py], 8.05 [1H, dd, *J*(H–H) = 8.5 Hz, *J*(H–H) = 1.0 Hz, CH, 6-quin], 8.01 [1H, ddd, *J*(H–H) = 8.5 Hz, *J*(H–H) = 7.2 Hz, *J*(H–H) = 1.3 Hz, CH, 7-quin], 7.74 [1H, ddd, *J*(H–H) = 8.1 Hz, *J*(H–H) = 7.0 Hz, *J*(H–H) = 1.0 Hz, CH, 8-quin], 7.51 [1H, ddd, *J*(H–H) = 7.3 Hz, *J*(H–H) = 5.4 Hz, *J*(H–H) = 1.0 Hz, CH, 5-py], 7.32 (2H, s, *m*–C₆H₂), 6.75 [1H, d, *J*(H–H) = 9.4 Hz, CH, 3-quin], 6.71 [1H, ddd, *J*(H–H) = 8.4 Hz, *J*(H–H) = 1.0 Hz, *J*(H–H) = 0.9 Hz, CH, 3-py], 2.47 (3H, s, *p*–CH₃), 2.07 (6H, s, *o*–CH₃). ¹³C NMR (CD₃OD): δ 155.27, 153.96, 146.01, 144.97, 144.17,

(*N*-(2,6-Diisopropyl)phenyl-*N,N*-(2,2'-diquinolyl)amine)hydrogen Tetrafluoroborate (**3**)

In a 25 mL round bottom flask, (2,6-ⁱPr₂C₆H₃)N(quin)₂ (0.431 g, 1.0 mmol) was dissolved in MeOH (15 mL). With stirring, KBF₄ (0.130 g, 1.0 mmol) dissolved in dilute HCl (5 mL) was slowly added. The mixture was allowed to stir for 30 min, followed by extraction with

143.17, 139.68, 138.21, 134.77, 133.42, 132.57, 129.84, 128.75, 125.59, 123.43, 121.78, 115.40, 113.67, 21.42, 17.44.

(N-(Phenyl)-N-(2-pyridyl)-N-(2-quinolyl)amine)dichloro Copper(II) (5)

[Cu(MeCN)₄]BF₄ (0.157 g, 0.5 mmol) and PhN(py)quin (0.149 g, 0.5 mmol) were stirred together in tetraethylene glycol (2 mL) in a conical vial open to the atmosphere, until all solids had dissolved. Dilute HCl (2 mL) was then added to the mixture, turning the dark blue/green solution milky white. The mixture was then extracted with CH₂Cl₂ (2 × 5 mL), and the combined organic layers were allowed to evaporate. The resulting brown residue was taken up in MeOH (5 mL), and then filtered. Recrystallization by a very slow evaporation of MeOH solution yielded dark red plates suitable for diffraction. Yield: 48%. Mp (TGA; decomp.) 89–91 °C. FTIR (neat, ATR, cm^{−1}): 3555 (w, br), 3433 (m, v br), 3111 (w, aromatic $\nu_{\text{C}-\text{H}}$), 3088 (w, aromatic $\nu_{\text{C}-\text{H}}$), 3061 (w, aromatic $\nu_{\text{C}-\text{H}}$), 3048 (w, aromatic $\nu_{\text{C}-\text{H}}$), 3023 (w, aromatic $\nu_{\text{C}-\text{H}}$), 2919 (w, br), 1688 (m), 1604 (s), 1507–1428 (s, aromatic $\delta_{\text{C}=\text{C}}$), 1343 (s,

3° aromatic $\nu_{\text{C}-\text{N}}$), 1317 (m), 1255 (m), 1148 (m), 1077 (m), 822 (m), 764 (s).

Crystal Data

X-ray data for compounds **1–5** was collected on a Bruker SMART 1000 CCD diffractometer equipped with graphite monochromated Mo-K α radiation ($\lambda = 0.71073 \text{ \AA}$) and corrected for Lorentz and polarization effects. All data sets were collected at room temperature, with the exception of compound **2**, for which data was collected at 213 K. Samples were prepared by suspension in mineral oil, facilitating separation and selection of a single crystal, followed by sealing in a thin layer of epoxy resin and securing to the end of a glass fiber. Fibers were fastened onto brass pins and mounted onto a fixed- χ 4-axis goniometer head. Data collection and unit cell refinement were carried out according to established methods [5] using the program SMART [6]. The program SAINT [7] was used for data reduction, and absorption correction was applied using SADABS [8]. Pertinent details are given in Table 1. Heavy atom sites were located by Patterson methods in complex **5**, while all other structure solution was performed by direct methods. Models were refined using full-matrix

Table 1 Summary of X-ray diffraction data

Compound	1	2	3	4	5
Empir. formula	C ₂₇ H ₂₃ N ₃	C ₂₆ H ₂₂ N ₃	C ₃₀ H ₃₀ N ₃ BF ₄	C ₂₃ H ₂₂ N ₃ BF ₄	Cu ₄ C ₈₀ H ₆₀ N ₁₂ C ₁₈
MW	389.48	381.51	519.38	427.25	1727.2
Cryst. system	Monoclinic	Monoclinic	Orthorhombic	Monoclinic	Triclinic
Space group	P21/c	P21/c	Pbca	P21/c	P $\bar{1}$
<i>a</i> (Å)	14.058(3)	22.250(4)	13.886(3)	10.629(2)	9.706(2)
<i>b</i> (Å)	12.202(2)	8.628(2)	18.016(4)	18.489(4)	11.325(2)
<i>c</i> (Å)	12.831(3)	23.031(5)	21.347(4)	10.907(2)	17.322(4)
α (°)	—	—	—	—	98.28(3)
β (°)	104.61(3)	98.74(3)	—	92.88(3)	94.85(3)
γ (°)	—	—	—	—	91.83(3)
V (Å ³)	2129.8(8)	4370(2)	5340(2)	2140.6(7)	1875.6(7)
Z	4	8	8	4	1
Dcalc (g/cm ³)	1.215	1.16	1.292	1.326	1.529
μ (mm ^{−1})	0.072	0.069	0.095	0.103	1.458
2θ range (°)	3.00–58.14	1.86–58.08	3.82–56.64	3.84–55.12	2.38–58.14
No. collected	25579	52928	63544	25553	22968
No. ind. (Rint)	5339 (0.0775)	10869 (0.0484)	6620 (0.1919)	4934 (0.1101)	9003 (0.0880)
No. obsd. (F _o > 4.0σ F _c)	2705	6745	2009	1728	3802
R	0.0596	0.0514	0.0722	0.0551	0.0481
Rw	0.1453	0.1323	0.1635	0.1531	0.0946
Δρ _(max,min) (eÅ ^{−3})	0.218, −0.199	0.203, −0.195	0.171, −0.222	0.249, −0.221	0.548, −0.417
Weights	0.0779, 0.5859	0.0771, 0	0.0945, 0	0.0963, 0	0.0398, 0
CCDC No.	741964	779677	779679	779678	732508

least squares techniques [9]. Refinement was performed with anisotropic thermal parameters for all non-hydrogen atoms: shift/error less than 0.01. With the exceptions of the pyridyl-bound hydrogen atoms in **3** and **4**, which were located in the difference map and refined freely; all other hydrogen atoms were placed in calculated positions for T = 298 K in compounds **1** and **3–5** [C–H (methine) = 0.98 Å, C–H (methyl) = 0.96 Å, and C–H (aromatic) = 0.93 Å] and for T = 213 K in compound **2** [C–H (methine) = 0.99 Å, C–H (methyl) = 0.97 Å, and C–H (aromatic) = 0.94 Å], which were refined using a riding model with fixed isotropic displacement parameters. Neutral-atom scattering factors were taken from the usual source [10]. Refinement of positional and anisotropic displacement parameters led to convergence for all data. The program used for structure solution and refinement was SHELXTL Version 6.14 [11]. The program PLATON was employed for structural validation [12, 13], which led to use of the squeeze function for the refinement of **2**, free of residual electron density found present in solvent accessible voids. Selected bond lengths and angles are given in Tables **2**, **3** and **4**. Regarding the structures **3** and **4**, the ratio of observed to unique reflections is toward the lower-end of desirable, which is likely a consequence of room temperature data collection. The high R_{int} value observed in compound **3** (0.1919) likely results from a combination of the disordered anion (see below), data collection temperature, as well as a somewhat irregularly shaped crystal.

The BF₄[−] anion present in the crystal structure of compound **3** was found to have a 50:50 site occupancy disorder for all four fluorine atoms. The disorder, shown in Fig. 1, is a C₂ rotation about an axis slightly tilted off the B(1)–F(1) bond. For initial refinement cycles, similar distance restraints (SADI) were placed on all B–F and F–F distances, in addition to similar ADP restraints (SIMU) and rigid bond restraints (DELU) for all F atoms. Similar distance restraints were lifted for final refinement cycles.

Table 2 Selected bond lengths (Å) and angles (°) determined for RN(quin)₂

R	Mes (1)	2,6- ⁱ Pr ₂ C ₆ H ₃ (2) ^a
Na–Cpy/quin	1.412(3)	1.409(2), 1.418(2)
Na–Cquin	1.401(2)	1.411(2), 1.398(2)
Na–Carom	1.443(2)	1.451(2), 1.453(2)
C _{quin} /py–Na–Cquin	124.1(1)	122.2(1), 122.6(1)
C _{quin} /py–Na–Carom	117.1(1)	116.9(1), 117.5(1)
Cquin’–Na–Carom	118.8(1)	117.2(1), 119.2(1)
Σ[Ci_Na_Cj]	360	356.3, 359.4
ΔMPLN[quin/py_quin’]	44.9(1)	50.2(1), 42.0(1)
ΔMPLN[Ar_quin/py]	82.6(1)	84.8(1), 89.6(1)
ΔMPLN[Ar-quin’]	76.1(1)	75.4(1), 86.8(1)

^a Two unique conformers in the asymmetric unit

Table 3 Selected bond lengths (Å) and angles (°) for [H{RN(quin)₂}]BF₄

R	2,6- ⁱ Pr ₂ C ₆ H ₃ (3)	Mes (4)
N(1)–Cpy	1.413(4)	1.423(4)
N(1)–Cquin	1.391(3)	1.377(3)
N(1)–CAr	1.452(3)	1.451(3)
N···H ⁺	1.70(4)	1.80(3)
N···H ⁺	1.01(4)	0.92(3)
F···H ⁺	2.88(4)	2.58(3)
Cpy–N–Cquin	125.1(3)	125.8(2)
Cpy–N–CAr	118.3(2)	115.7(2)
Cquin–N–CAr	116.3(2)	118.6(2)
Npy–Cpy–Cpy’–Npy'	1.8(2)	3.2(2)
ΔMPLN[py_quin]	3.7(2)	4.0(1)
ΔMPLN[py_Ar]	89.4(2)	88.0(1)
ΔMPLN[quin_Ar]	86.4(2)	89.09(8)

Table 4 Selected bond lengths (Å) and angles (°) for compound **5**

Dimer	Monomer
Cu(1)–N(2)	1.985(3)
Cu(1)–N(3)	2.030(3)
Cu(1)–Cl(1)	2.275(1)
Cu(1)–Cl(1A)	2.560(1)
Cu(1)–Cl(2)	2.307(1)
N(1)–C(1)	1.411(5)
N(1)–C(6)	1.401(5)
N(1)–C(11)	1.454(5)
Cu(1)···Cu(1A)	3.613(1)
Cl(1)–Cu(1)–Cl(1A)	83.47(5)
Cl(1)–Cu(1)–Cl(2)	97.06(6)
Cl(1)–Cu(1)–N(2)	161.2(1)
Cl(1)–Cu(1)–N(3)	93.3(1)
Cl(2)–Cu(1)–N(2)	99.4(1)
Cl(2)–Cu(1)–N(3)	97.06(6)
N(2)–Cu(1)–N(3)	85.2(1)
Cu(1)–Cl(1)–Cu(1A)	96.53(5)
C(1)–N(1)–C(6)	124.9(4)
C(1)–N(1)–C(15)	117.1(3)
C(6)–N(1)–C(15)	117.7(3)
Cu(1)···N(1)–C(15)	145.6(3)
N(2)–C(1)–C(6)–	1.0(3)
ΔMPLN[py_quin]	33.3(1)
ΔMPLN[py_Ar]	78.6(1)
ΔMPLN[quin_Ar]	68.3(1)
N(5)–C(21)–C(26)–	
N(6)	
ΔMPLN[py_quin]	28.3(2)
ΔMPLN[py_Ar]	81.2(2)
ΔMPLN[quin_Ar]	73.6(1)

Similarly, the BF₄[−] anion present in the crystal structure of **4** was found to have a site occupancy disorder (45:55) for three of the four fluorine atoms. The disorder, shown in

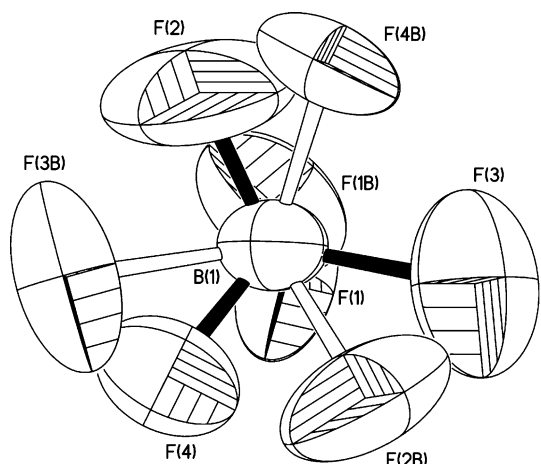


Fig. 1 Structure for the BF_4^- anion in $[\text{H}\{(2,6\text{-iPr}_2\text{C}_6\text{H}_3)\text{N}(\text{quin})_2\}]\text{BF}_4$ (**3**) with both parts of the disorder present. For clarity, thermal ellipsoids are shown at the 25% level

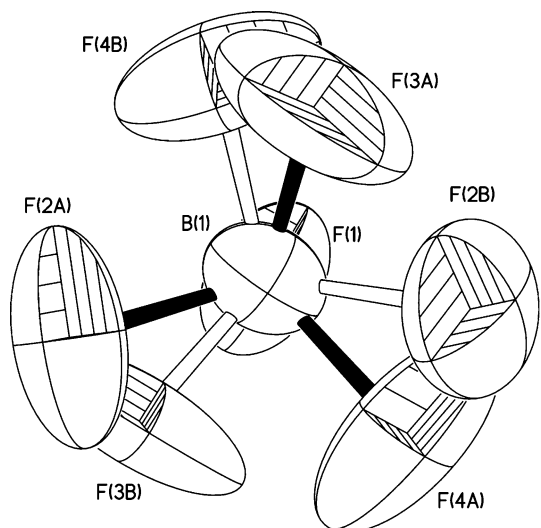


Fig. 2 Structure for the BF_4^- anion in $[\text{H}\{\text{MesN}(\text{py})\text{quin}\}]\text{BF}_4$ (**4**) with both parts of the disorder present. For clarity, thermal ellipsoids are shown at the 25% level

Fig. 2, is a C_2 rotation about the axis of the $\text{B}(1)\text{--F}(1)$ bond. For initial refinement cycles, similar distance restraints (SADI) were placed on all $\text{B}\text{--F}$ and $\text{F}\text{--F}$ distances, in addition to similar ADP restraints (SIMU) and rigid bond restraints (DELU) for all F atoms. All restraints were lifted for final refinement cycles.

Results and Discussion

Free Ligands

The structure of the aryl-functionalized *bis*(2-quinolyl)amine, $\text{MesN}(\text{quin})_2$ (**1**) and the (2-pyridyl)(2-quinolyl)amine, $(2,6\text{-iPr}_2\text{C}_6\text{H}_3)\text{N}(\text{py})\text{quin}$ (**2**) are shown in

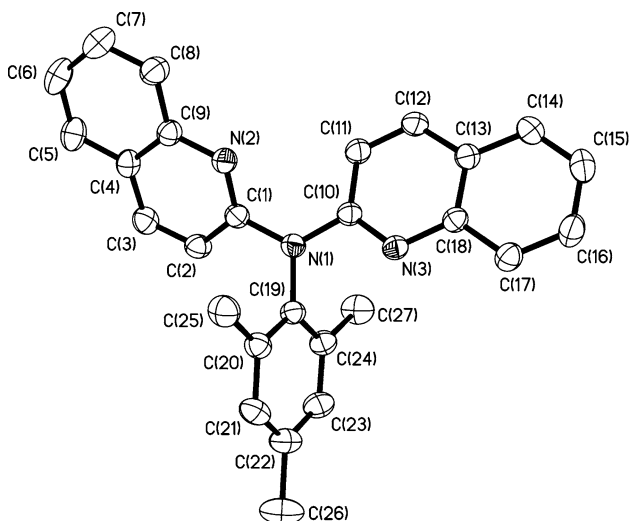


Fig. 3 Molecular structure of $\text{MesN}(2\text{-quin})_2$ (**1**). Thermal ellipsoids are shown at the 30% level, and all hydrogen atoms are omitted for clarity

Figs. 3 and 4, respectively. Selected bond lengths and angles are given in Table 2. As observed in similar compounds [2, 3], both **1** and **2** crystallize in a three-bladed propellar conformation, having nearly planar geometry about the central amine nitrogen atom. Compound **2** was found to crystallize with two unique conformations in the asymmetric unit (see Fig. 4), having most prominent differences in the orientation of the quinolyl heterocycles with respect to the rest of the molecule. Specifically, rotation of the quinolyl group 180° about the $\text{N}_{\text{amine}}\text{--C}_{\text{quin}}$ bond in the first conformer approaches the conformation of the second. A second apparent difference regarding the quinolyl heterocycles is seen in the mean plane angle difference (ΔMPLN), with the respective pyridyl ring, which is larger in the first conformer [$50.2(1)^\circ$] than in the second [$42.0(1)^\circ$]. These are both significantly larger than those observed in the phenyl derivative [$31.9(1)$ and $31.3(1)^\circ$], while the $\text{MesN}(\text{py})\text{quin}$ free ligand yields a value [$48.5(2)^\circ$] [2] more akin to that in **2a**.

The analogous ΔMPLN angle in Mes-dqa (**1**) between the two heterocycles is observed to be intermediate [$44.9(1)^\circ$] between **2a** and **2b**, while the previously reported [3] $2,6\text{-iPr}_2\text{Ph-dqa}$ compound exhibits a value [$41.2(1)^\circ$] closer to that of **2b**. Furthermore, the ΔMPLN values between pyridyl rings in structurally similar Ar-dpa ligands (Ar = Mes, 2,6-Et₂Ph, 2-iPrPh, 2,6-iPr₂Ph, 1-naph, [1] and Ph [14]) are found to exhibit values [$40.7(1)$ – $48.7(1)^\circ$] primarily within the range spanned by the two extremes seen in **2**. The only dipyrindyl analogs that clearly lie outside of this range are those reported with substitution in the *para*- position, $(p\text{-OMe})\text{Ph-dpa}$ and $(p\text{-CN})\text{Ph-dpa}$, having values of $57.7(1)$ and $49.2(1)^\circ$ in the former, and $65.3(1)^\circ$ in the latter [14].

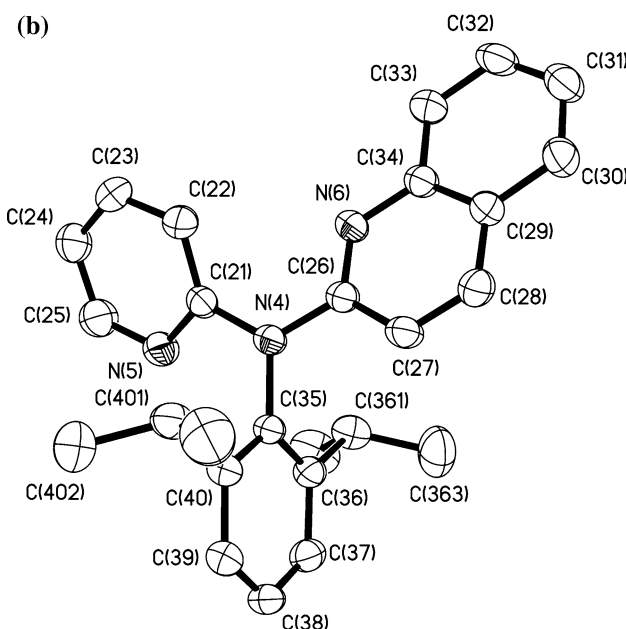
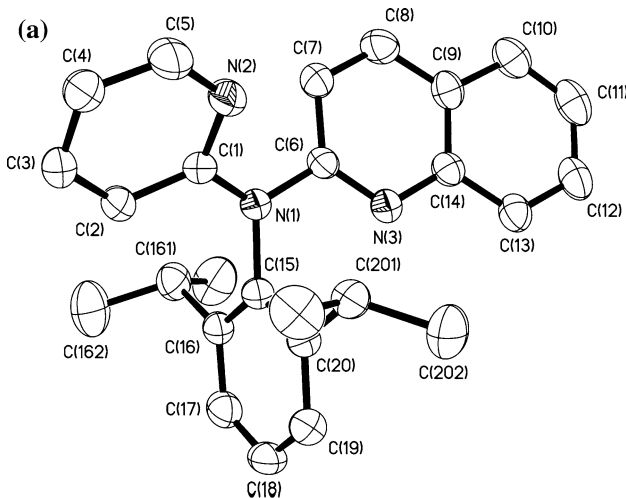


Fig. 4 Molecular structure of the two unique conformers of $(2,6\text{-}i\text{Pr}_2\text{C}_6\text{H}_3)\text{N}(2\text{-py})(2\text{-quin})$ (**2**) present in the asymmetric unit. Thermal ellipsoids are shown at the 30% level, and all hydrogen atoms attached to carbon are omitted for clarity

A further easily perceptible difference between the conformers of **2** is seen in the geometry about the amine nitrogen atom. More specifically, the deviation from planarity, i.e., the departure from 360° of the sum of the three $\text{C}_i\text{--N}_{\text{amine}}\text{--C}_j$ bond angles ($\Sigma_{\text{Ci--Na--Cj}}$), in **2a** [$356.3(1)^\circ$] is significantly larger than that in **2b** [$359.4(1)^\circ$] (see Table 2). Surprisingly, the value in **2a** seems to exist at the lower extreme for $\Sigma_{\text{Ci--Na--Cj}}$, in structurally similar compounds, including the other aforementioned $\text{ArN}(\text{py})\text{quin}$ compounds ($\text{Ar} = \text{Ph}$ and Mes), the diquinolyl compounds, **1** and $2,6\text{-}i\text{Pr}_2\text{Ph}\text{-dqa}$, as well as all of the Ar-dpa ligands. In fact, of those mentioned above, the only other compound that features a $\Sigma < 359^\circ$ is the $(p\text{-CN})\text{Ph-dpa}$ derivative, in which the angles sum to 357.7° .

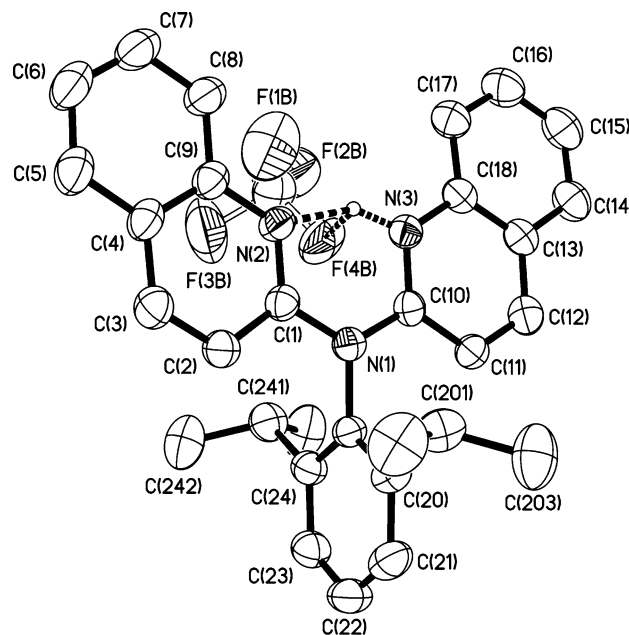


Fig. 5 Molecular structure of the acid salt $[\text{H}\{(2,6\text{-}i\text{Pr}_2\text{C}_6\text{H}_3)\text{N}(2\text{-quin})\}_2]\text{BF}_4$ (**3**). Thermal ellipsoids are shown at the 30% level, and all hydrogen atoms attached to carbon are omitted for clarity

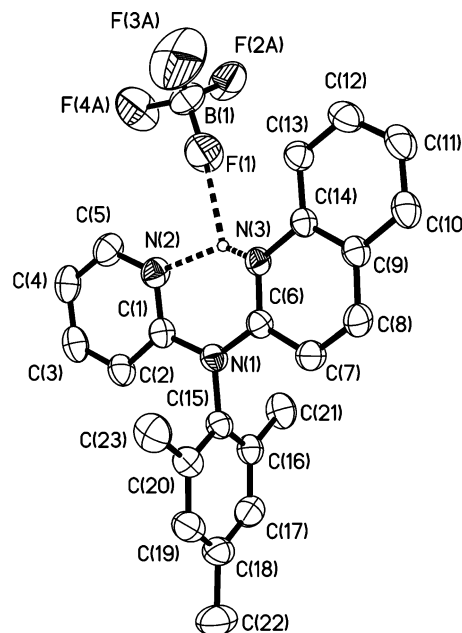


Fig. 6 Molecular structure of the acid salt $[\text{H}\{\text{MesN}(\text{2-py})(\text{2-quin})\}]\text{BF}_4$ (**4**). Thermal ellipsoids are shown at the 30% level, and all hydrogen atoms attached to carbon are omitted for clarity

HBF₄ Acid Salts of ArN(py/quin)(quin)

The structures of acid salts $[\text{H}\{(2,6\text{-}i\text{Pr}_2\text{C}_6\text{H}_3)\text{N}(\text{quin})_2\}]\text{BF}_4$ (**3**) and $[\text{H}\{\text{MesN}(\text{py})\text{quin}\}]\text{BF}_4$ (**4**) are shown in Figs. 5 and 6, respectively. Selected bond lengths and angles are given in Table 3. Coordination of the proton is observed to be asymmetric in both complexes, having

N···H distances ranging from 0.92(3) to 1.80(3) Å. The protons also appear to be loosely associated with the BF_4^- anions [$\text{H} \cdots \text{F} = 2.88(4)$ and 2.58(3) Å]. The longer H···F distance and smaller N–H···F angle (from the shorter N–H interaction) in **3** [115(3)°] are indicative of a weaker H-bonding interaction than observed in **4** [N–H···F = 134(2)°]. This is to be expected, as the greater steric occupation of a second quinolyl group prevents the anion from approaching from the side, as seen in the case of **4**, where the anion occupies a pocket on the pyridyl side of the molecule.

As a result of the bidentate, albeit asymmetric, coordination, the two heterocycles are forced to adopt a nearly coplanar geometry [$\Delta\text{AMPLN}_{[\text{py}/\text{quin}-\text{quin}]} = 3.7(2)^\circ$ and 4.0(1)°; $\text{N}_{\text{py}}-\text{C}_{\text{py}/\text{quin}} \cdots \text{C}_{\text{py}'}/\text{N}_{\text{quin}'} = 1.8(2)$ and 3.2(2)° respectively], which is clearly unfavorable sterically, considering the ΔAMPLN values in the free ligands (see above). The $\text{N}_a-\text{C}_{\text{quin}/\text{py}}$ and $\text{N}_a-\text{C}_{\text{quin}}$ distances in both compounds exhibit larger asymmetry [1.413(4) and 1.391(3) Å in **3**; 1.423(4) and 1.377(3) Å in **4**] compared to the analogous free ligands, each of which feature nearly identical bond lengths to both heterocyclic carbon atoms [1.400(2) and 1.410(2) Å in 2,6-ⁱPr₂Ph-dqa; 1.400(4) and 1.406(4) Å in MesN(py)quin]. This is consistent with protonation of one quinolyl moiety rather than a symmetric chelation of the proton. This degree of asymmetry in proton chelation is not observed in the structurally similar HClO_4 and HBr salts of $\text{HN}(\text{py})_2$ [1.362(6) and 1.362(6) Å; 1.33 and 1.40 Å, respectively] [15], or the $[\{\text{HN}(\text{py})_2\}_2\text{H}]\text{CoCl}_4$ complex [1.33(3) and 1.36(3) Å] [16].

$\pi \cdots \pi$ stacking between quinolyl rings of adjacent molecules is evident in the crystal packing diagram of **3** (Fig. 7), with a distance of 3.680(2) Å between nearly parallel [5.1(2)°] rings. Similarly, crystal packing in **4** shows a stacking interaction between quinolyl rings [3.638(2) Å; 0°].

Copper(I) Complex of PhN(py)quin

The copper complex $\text{Cu}[\text{PhN}(\text{py})\text{quin}]\text{Cl}_2$ (**5**) is prepared by the reaction of $[\text{Cu}(\text{MeCN})_4]\text{BF}_4$ with PhN(py)quin in tetraethylene glycol in the presence of dilute HCl. The solid state structure of compound **5** as determined by X-ray crystallography was found to exhibit two crystallographically unique conformers in the asymmetric unit. The molecular structures of the two independent molecules in the asymmetric unit are shown in Fig. 8; selected bond lengths and angles are given in Table 4. Although it is not unusual to observe two independent molecules within a given asymmetric unit, it is rather surprising to see the degree to which the geometries differ about the copper atoms for each conformer in **5**. Specifically, Cu(1) exists in the dimeric form (**III**) (Fig. 8a) as is observed for the PhN(py)₂ analog. Although Cu(2) may also seem to be a

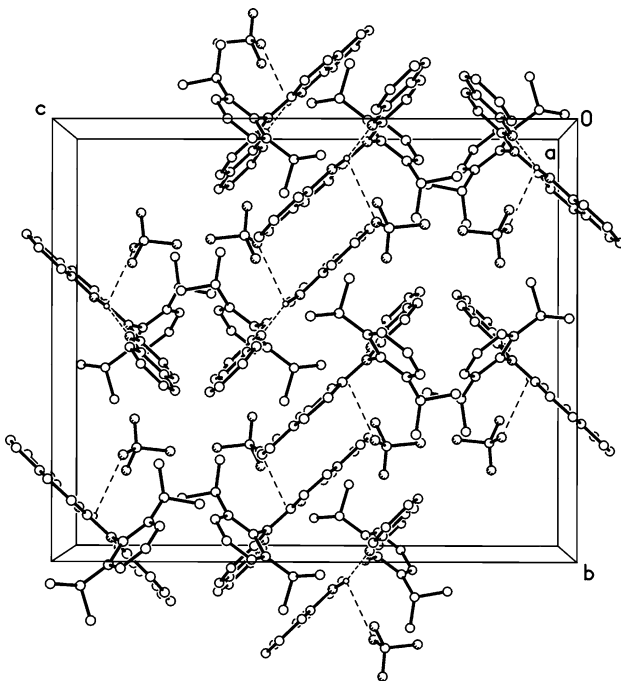
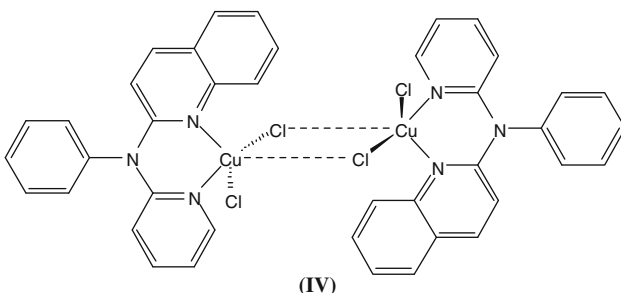
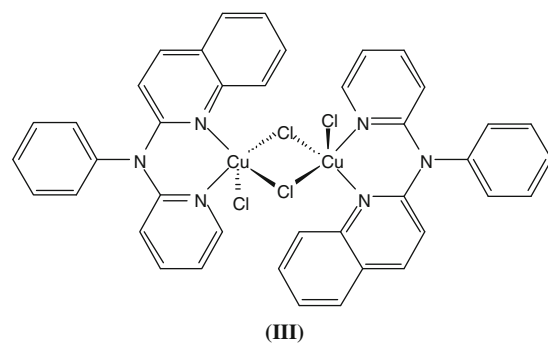


Fig. 7 Crystal packing diagram of $[\text{H}\{(2,6-\text{iPr}_2\text{C}_6\text{H}_3)\text{N}(2\text{-quin})_2\}]\text{BF}_4$ (**3**) (viewed along the *c*-axis) highlighting $\pi \cdots \pi$ stacking between heterocycles of adjacent molecules, as well as the interaction between the pyridyl bound H atom and the BF_4^- anion

dimer, considering the proximity of a symmetry related Cu(2)-unit (Fig. 8b), the intramolecular distances and the geometry about Cu(2) are more consistent with a monomeric form (**IV**).



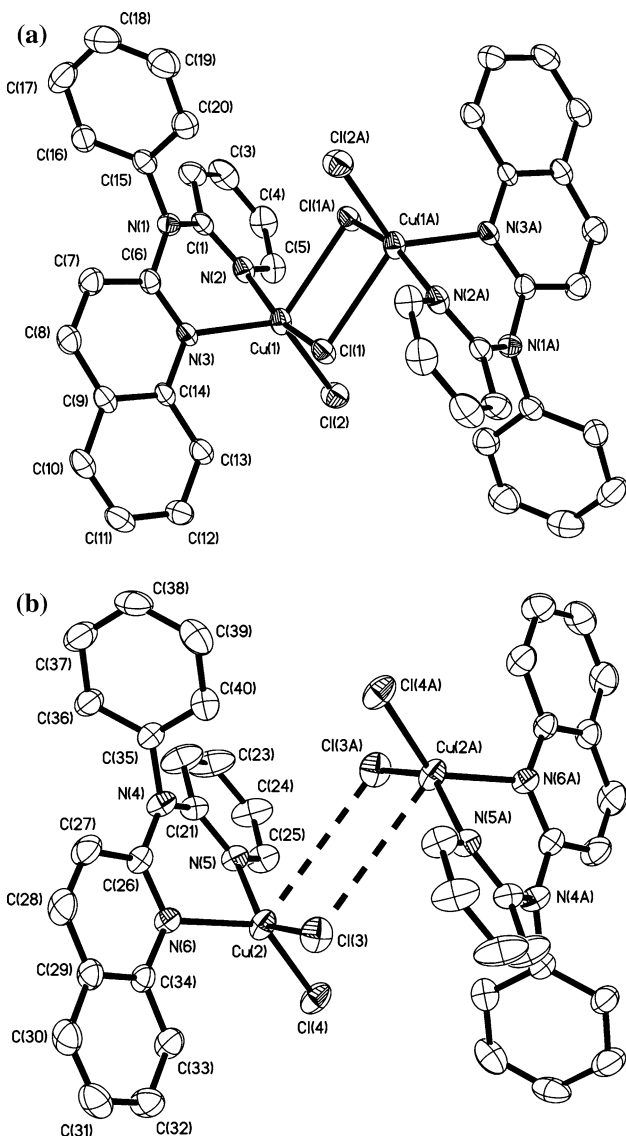


Fig. 8 Molecular structures of **a** the dimeric and **b** monomeric forms of $\text{Cu}[\text{PhN}(\text{py})\text{quin}]Cl_2$ (**5**). The latter shows the very weak interaction with a neighboring molecule. Thermal ellipsoids are shown at the 30% level, and all hydrogen atoms are omitted for clarity

The coordination geometry about Cu(1) in compound **5** is that of a distorted trigonal bipyramidal, with the axial positions occupied by the pyridyl nitrogen and one of the bridging chlorides. The *trans*-angle [161.2(1) $^\circ$] is slightly smaller than the range seen for the related RN(py)₂ derivatives [176.18(5)–178.2(1) $^\circ$] [1]. The trigonal bipyramidal coordination spheres observed in these bridged dimers is also observed in the structurally related compounds $\{\text{Cu}[\text{CH}_2(\text{py})_2]\text{Cl}_2\}_2$ [17], $[\text{Cu}(o\text{-phen})\text{Cl}_2]_2$ [18], and $[\text{Cu}(\text{bipy})\text{Cl}_2]_2$ [19]. In contrast, the geometry about Cu(2) is much closer to that expected for a square planar monomer typical for Cu(II) compounds, with the *trans*-angles being 141.8(1) $^\circ$. A comparison of the inner

coordination sphere of the copper atoms is shown in Fig. 9.

The bridging Cu–Cl distances associated with Cu(1), 2.270(1) and 2.554(1) \AA , are similar to those observed for $[\text{Cu}\{\text{RN}(\text{py})_2\}\text{Cl}_2]_2$ [2.261(1)–2.296(2) \AA and 2.596(2)–2.7299(7) \AA , respectively], where R = Ph, 2ⁱPrPh, and 1-naph. Furthermore, they are consistent with the hybridization associated with the trigonal bipyramidal structure (i.e., the axial = p and equatorial = sp^2) as well as the relative *trans*-influences of the chloride and pyridyl ligand. A comparison of the distances for Cu(2) shows that while one of the distances to the “bridging” chloride is reasonable [2.232(1) \AA] the other is significantly longer than reasonable for a covalent Cu–Cl bond [3.795(1) \AA]. In fact both Cu(2)–Cl(3) and Cu(2)–Cl(4) distances are within the range expected for terminal interactions.

A measure of the relative asymmetry of the bridging unit can be defined as the $\Delta\text{Cu–Cl}$. For Cu(1) in **5** this is 0.284 \AA , while for $[\text{Cu}\{\text{RN}(\text{py})_2\}\text{Cl}_2]_2$ the values are as follows: 0.4544 \AA (R = Ph); 0.3 \AA (R = ⁱPrC₆H₄), and 0.437 and 0.419 \AA (R = 2-naph). Thus, the dimeric form of compound **5** is actually more symmetrical than the RN(py)₂ derivatives. By contrast, the asymmetry of the distances associated with Cu(2) is 1.563 \AA : over three times that of the dimeric compounds. If we agree that Cu(2) is closer to a monomeric square planar geometry then it appears that compound **5** crystallizes in both dimeric and monomeric forms in the same asymmetric unit. The crystal packing diagram for compound **5** (Fig. 10) clearly shows the difference in Cu–Cu distances between the two forms.

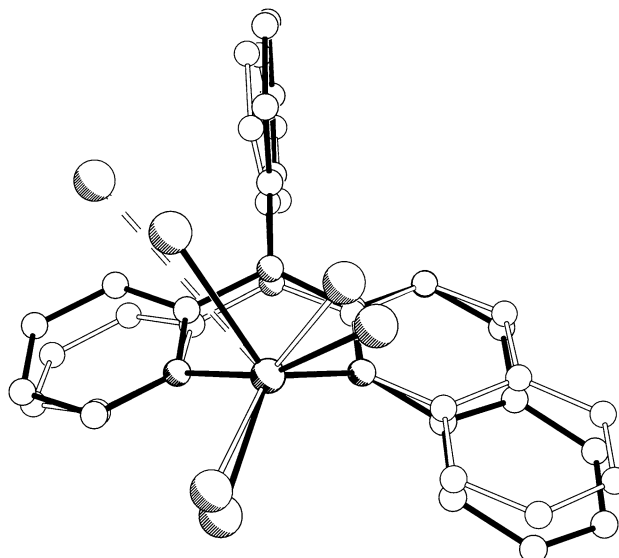


Fig. 9 Partial inner coordination spheres of monomer (open bonds) and dimer (solid bonds) in $\text{Cu}[\text{PhN}(\text{py})\text{quin}]Cl_2$ (**5**), which have been superimposed to highlight geometrical differences

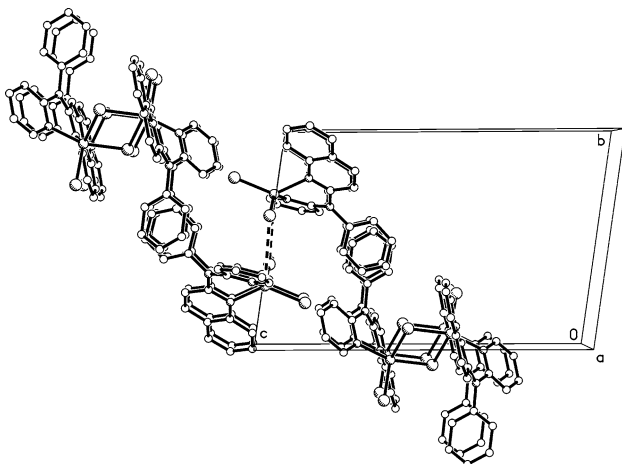


Fig. 10 Crystal packing of $\text{Cu}[\text{PhN}(\text{py})\text{quin}]\text{Cl}_2$ (**5**), viewed along the c -axis, highlighting packing differences between different forms

We propose that the presence of both monomeric and dimeric forms suggest that the energetic difference between each form is comparable to the crystal packing forces observed in the solid state. We have previously observed monomer/dimer disorder where crystal packing forces dominate allowing for either conformation [20].

Conclusions

Two novel *bis*(heterocyclic) ligands, $\text{MesN}(2\text{-quin})_2$ (**1**) and $2,6\text{-}^{\text{i}}\text{PrPh}_2\text{N}(2\text{-py})(2\text{-quin})$ (**2**), have been prepared and characterized. The structure of the diquinolyl compound, **1**, exhibits structural features similar to those in the $2,6\text{-}^{\text{i}}\text{Pr}_2$ -analog. In contrast, the (pyridyl)(quinolyl)amine compound, **2**, yielded two unique conformers in which the geometries differed tremendously. Interestingly, the geometry of the first conformer about the amine nitrogen deviates from planarity to a greater degree than any previously reported, structurally similar compound, including several di(2-pyridyl), (2-pyridyl)(2-quinolyl), and di(2-quinolyl)amines. The acid salts of the structurally similar ligands $2,6\text{-}^{\text{i}}\text{PrPh}_2\text{-dqa}$ (**3**) and Mes-pqa (**4**) were both observed to chelate the HBF_4^- proton in an asymmetric fashion to a degree that has not been observed previously [compared to *bis*(2-pyridyl)amines]. The chelation of the proton results in sterically unfavorable structures having nearly coplanar heterocycles. Not surprisingly, the BF_4^- anion in **3** exhibits a weaker interaction with the nitrogen chelated proton, which is a direct result of added sterics. The copper complex of the $\text{PhN}(2\text{-py})(2\text{-quin})$ ligand resulted in the formation of a dimeric structure rather similar to those observed in the Ar-dpa analogs; however, this dimeric compound, **5a**, was seen to co-crystallize with

the monomeric form (**5b**), in the same asymmetric unit of the crystal lattice. Such a phenomenon is suggestive that the relative energy difference between the two is on the same order as the crystal packing forces present.

Supplementary Material

CCDC no.'s 741964 (**1**), 779677 (**2**), 779679 (**3**), 779678 (**4**) and 732508 (**5**) contain the supplementary crystallographic data for this paper. These data can be obtained free of charge via www.ccdc.cam.ac.uk/conts/retrieving.html or from the Cambridge Crystallographic Data Centre, 12, Union Road, Cambridge CB2 1EZ, United Kingdom; fax: (+44)-1223-336-033; e-mail: deposit@ccdc.cam.ac.uk.

Acknowledgments Financial support for this work is provided by Trans Ionics Corporation. The Robert A. Welch Foundation is acknowledged for funding of the Texas Center for Crystallography at Rice University.

References

- Allen JJ, Hamilton CE, Barron AR (2010) Dalton Trans 39:11451–11468
- Allen JJ, Hamilton CE, Barron AR (2010) J Chem Cryst 40:137–144
- Allen JJ, Hamilton CE, Barron AR (2010) J Chem Cryst 40:130–136
- Hathaway BJ, Holah DJ, Postlethwaite JD (1961) J Chem Soc 3215
- Ruhl S, Bolte M (2000) Z Kristallogr 215:499
- Bruker (2003) SMART v5.63. Bruker AXS Inc., Madison
- Bruker (2003) SAINT v6.45. Bruker AXS Inc., Madison
- Sheldrick GM (2008) SADABS. University of Göttingen, Göttingen
- Sheldrick GM (2008) Acta Cryst A64:112–122
- Allen FH, Kennard O, Watson DG, Brammer L, Orpen AG, Taylor R (1995) In: Wilson AJC (ed) International tables for crystallography, vol C. Kluwer, Dordrecht, pp 685–706
- Sheldrick GM (2000) SHELXTL v6.14. Bruker AXS Inc., Madison
- Spek AL (2008) PLATON. Molecular Geometry Program, Utrecht
- Spek AL (2003) J Appl Cryst 36:7–13
- Yang JS, Lin YD, Lin YH, Liao FL (2004) J Org Chem 69:3517
- Junk PC, Lu W, Semenova LI, Skelton BW, White AHZ (2006) Anorg Allg Chem 632:1303
- Cotton FA, Daniels LM, Jordan GT, Murillo CA (1998) Polyhedron 17:589
- Spodine E, Manzur J, Garland MT, Fackler JP, Staples RJ, Trzcinska-Bancroft B (1993) Inorg Chim Acta 203:73
- Viossat B, Gaucher JF, Mazurier A, Selkti M, Tomas A (1998) Z Kristallogr 213:329
- Kostakis GE, Norlander E, Haukka M, Plakatouras JC (2006) Acta Cryst E62:m77
- Healy MD, Gravelle PW, Mason MR, Bott SG, Barron AR (1993) J Chem Soc Dalton Trans 441–454